

ARTIFICIAL NEURAL NETWORK-BASED ROBOTICS

A Thesis

presented to

the Faculty of California Polytechnic State University,

San Luis Obispo

In Partial Fulfillment

of the Requirements for the Degree

Master of Science in Electrical Engineering

by

Justin Ng

June 2018

© 2018  
Justin Ng  
ALL RIGHTS RESERVED

## COMMITTEE MEMBERSHIP

TITLE: Artificial Neural Network-Based Robotics

AUTHOR: Justin Ng

DATE SUBMITTED: June 2018

COMMITTEE CHAIR: Andrew Danowitz, Ph.D.  
Assistant Professor of Electrical Engineering

COMMITTEE MEMBER: Xiao-Hua Yu, Ph.D.  
Professor of Electrical Engineering

COMMITTEE MEMBER: Fred W. DePiero, Ph.D.  
Professor of Electrical Engineering

## ABSTRACT

Artificial Neural Network-Based Robotics

Justin Ng

Artificial neural networks (ANNs) are highly-capable alternatives to traditional problem solving schemes due to their ability to solve non-linear systems with a non-algorithmic approach. The applications of ANNs range from process control to pattern recognition and, with increasing importance, robotics. This paper demonstrates continuous control of a robot using an actor-critic algorithm based on deep deterministic policy gradients (DDPG) originally conceived by Google DeepMind. The robot performs tasks such as locomotion within an enclosed area and object transportation. The paper also details the robot design process and explores the challenges of implementation in a real-time system.

## ACKNOWLEDGMENTS

Thanks to:

- Everyone for everything.

## TABLE OF CONTENTS

	Page
LIST OF TABLES . . . . .	vii
LIST OF FIGURES . . . . .	viii
CHAPTER	
1 Introduction . . . . .	1
1.1 Cal Poly Roborodentia . . . . .	1
2 Mechanical Design . . . . .	3
2.1 Introduction . . . . .	3
2.2 Base Platform . . . . .	6
2.3 Shooting Mechanism . . . . .	6
2.4 Ball Hopper . . . . .	8
2.5 Control Unit . . . . .	8
3 Electrical Design . . . . .	9
4 Firmware Design . . . . .	10
5 Software . . . . .	11
5.1 Definitions and Assumptions . . . . .	11
5.2 Kalman Filters . . . . .	11
5.2.1 Algorithm . . . . .	12
5.2.2 Design . . . . .	13
6 Neural Network Design . . . . .	15
7 Conclusion . . . . .	16
BIBLIOGRAPHY . . . . .	17
APPENDICES	

## LIST OF TABLES

Table	Page
2.1 Roborodentia Mechanical Requirements . . . . .	3

## LIST OF FIGURES

Figure	Page
1.1 Roborodentia Field [1] . . . . .	2
2.1 Full Robot Render – Isometric View . . . . .	4
2.2 Full Robot Render – Top View . . . . .	4
2.3 Full Robot Render – Front View . . . . .	5
2.4 Full Robot Render – Right View . . . . .	5
2.5 Shooting Mechanism – Exploded View . . . . .	7
2.6 Shooting Mechanism – Top View . . . . .	7
2.7 Shooting Mechanism – Cross Section View . . . . .	8

# Chapter 1

## INTRODUCTION

**Note:** All project files can be found at <https://www.github.com/okayjustin/roborodentia2017>

### 1.1 Cal Poly Roborodentia

The robot is designed to compete in the 2018 Cal Poly Roborodentia, the university's annual intramural robotics competition, and thus conforms to its particular specifications and requirements. Briefly, competitors must produce autonomous robots to collect and fire Nerf Rival Balls into nets to win points. A drawing of the field is shown below in Figure 1.1. Two robots compete separately in each half so the effective field is a 4' wide by 8' long area enclosed by 4" walls. 1 inch PVC tubes along the 4' walls hold the balls which the robots fire into rectangular nets located along the 8' wall. The rules provide additional restrictions on robot dimensions, capabilities, and other aspects, to be covered specifically in the following chapters.

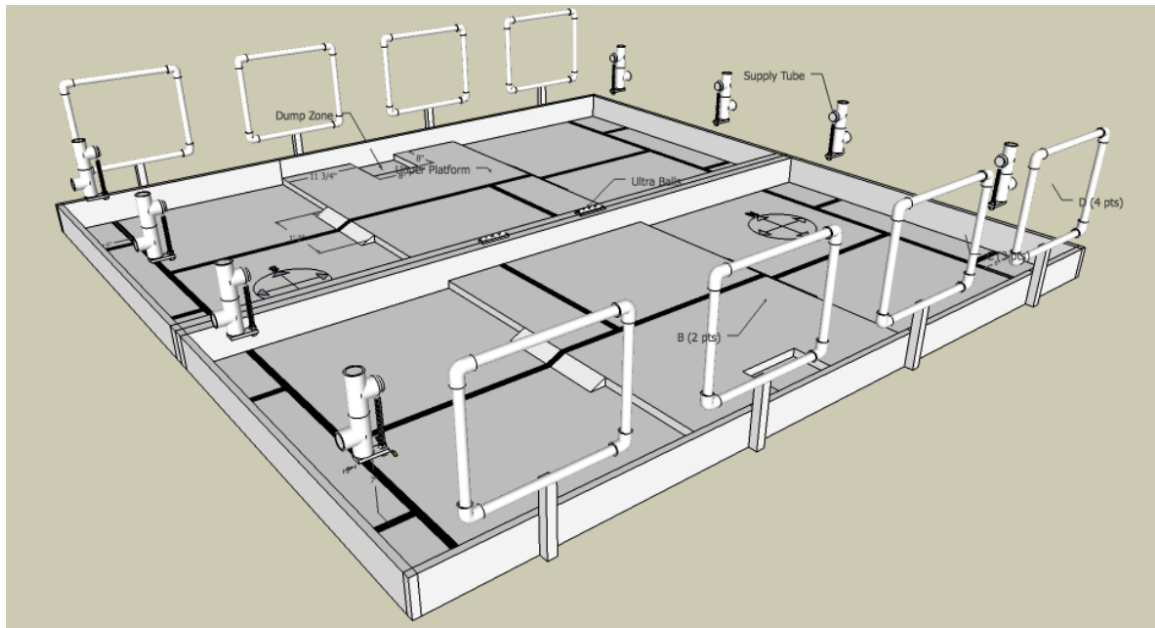


**Figure 1.1: Roborodentia Field [1]**

## Chapter 2

### MECHANICAL DESIGN

#### 2.1 Introduction

The robot meets the design specification shown in Table 2.1. It consists of four subassemblies: the base platform, shooting mechanism, ball hopper, and control unit. Each section was first modeled in SolidWorks, an industry-standard solid modeling CAD program. The designed parts were then fabricated using a laser cutter or 3D printer and assembled with metric hardware. Figures 2.1 through 2.4 show standard view renders of the robot.

**Table 2.1: Roborodentia Mechanical Requirements**

Contest Requirement
1 Maximum footprint of 12" x 14" or smaller at start of match but may expand up to 14" x 17" during match.
2 Maximum height of 14" at start of match but no restriction during match.
3 Robot may not disassemble into multiple parts.
4 Robot may not be airborne.
5 Shooting mechanisms may not accelerate balls past 50 feet per second.

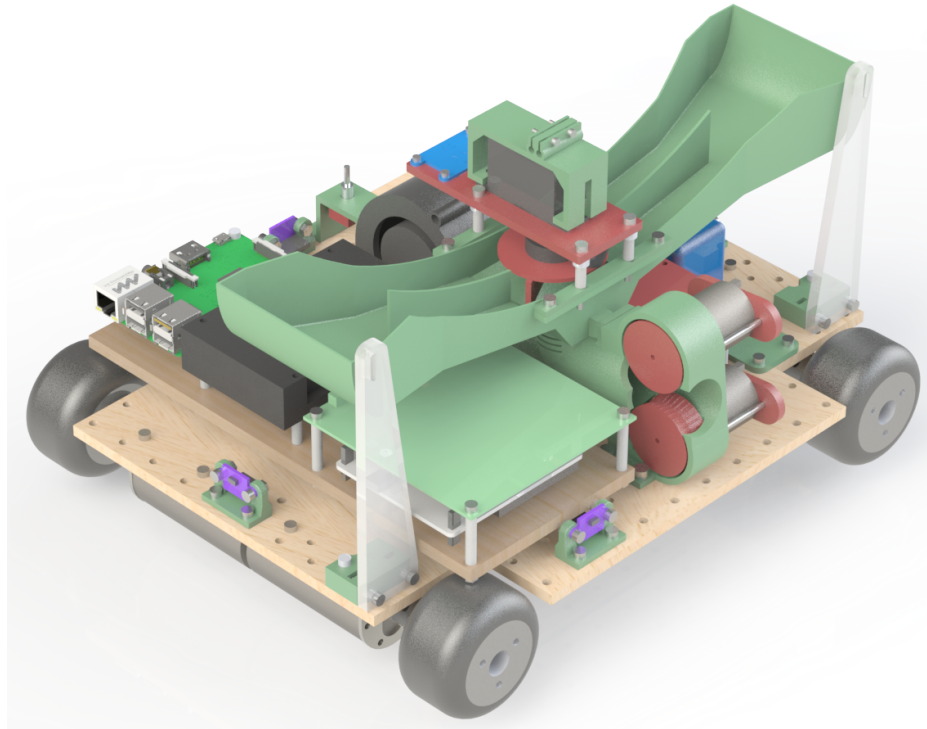


**Figure 2.1:** Full Robot Render – Isometric View

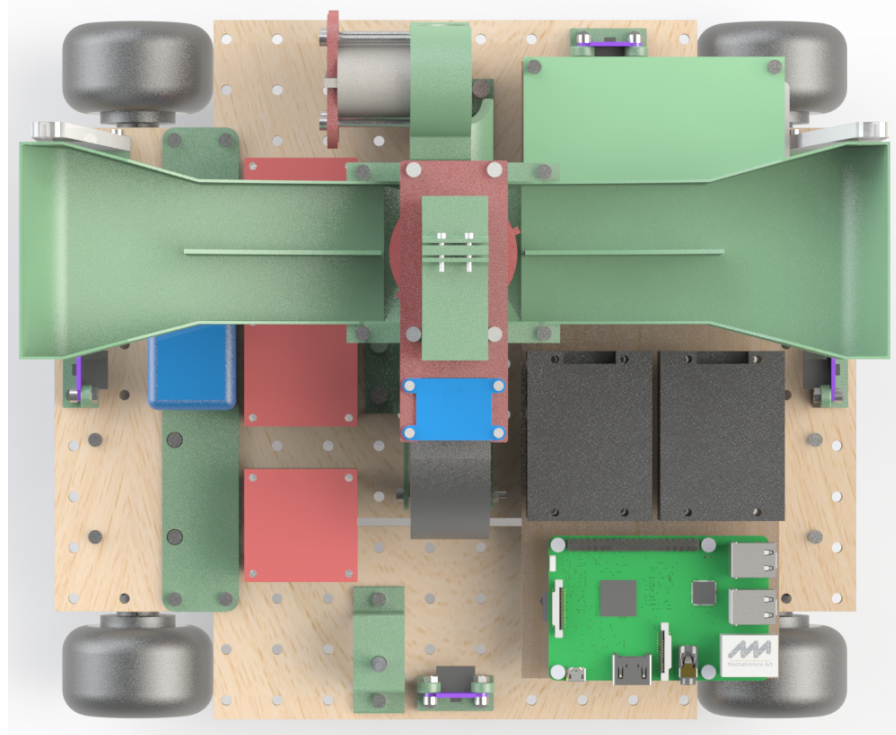


**Figure 2.2:** Full Robot Render – Top View

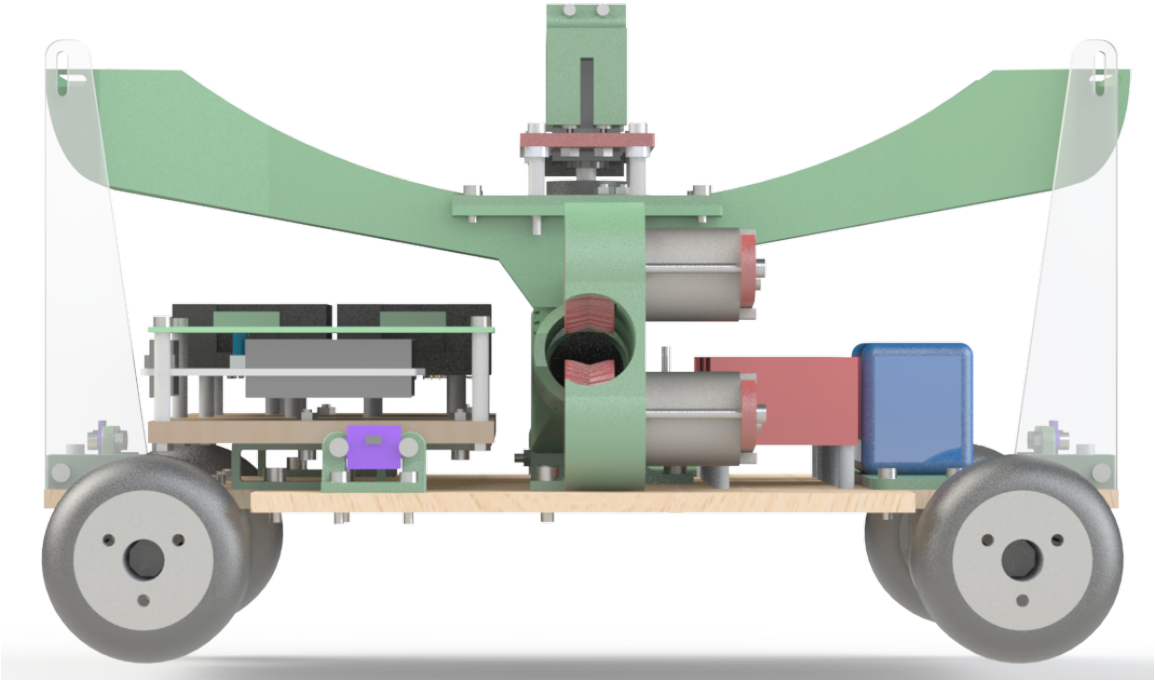


Figure 2.3: Full Robot Render – Front View

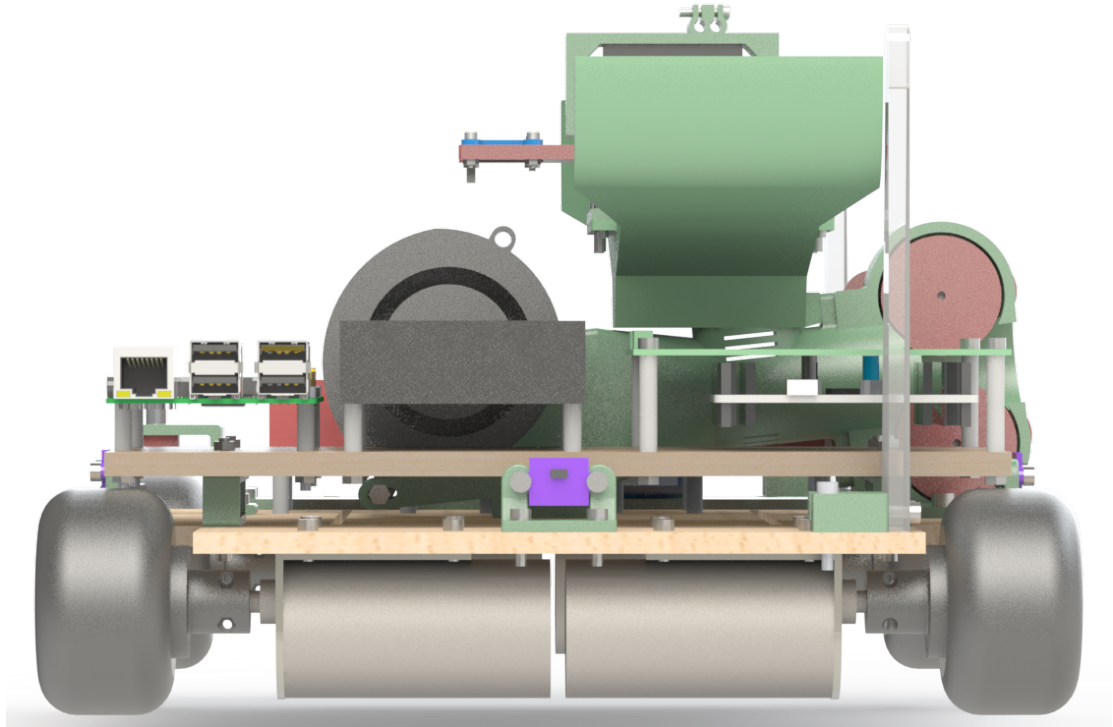


Figure 2.4: Full Robot Render – Right View

## 2.2 Base Platform

## 2.3 Shooting Mechanism

The shooting mechanism naturally takes inspiration from the official Nerf Rival Blaster toys since the manufacturer specifically optimized them to fire Nerf Rival balls in a way similar to baseball pitching machines. Figure 2.5 shows an exploded view of the subassembly while Figure 2.6 displays the top view. The mechanism consists of two sections: the **barrel** (leftmost green part in Figure 2.5) and the **wheel housing** (rightmost green part in Figure 2.5). Both parts were fabricated using a fused deposition modeling (FDM) 3D printer as the geometries are highly complex. The shooting mechanism was designed as two separate components versus a unibody design to allow each half to be fabricated with optimal print direction, strength, and finish quality.

The barrel The ball enters the mechanism through a top chute perpendicular to the barrel by force of gravity. As the ball falls into the barrel, a high-pressure centrifugal (or blower fan) at the back of the barrel pushes it towards the rotating wheels which grab onto the ball and accelerate it out of the shooting mechanism. As seen in Figure 2.7, the barrel slightly narrows in the area behind the top chute to prevent the ball from rolling backwards towards the blower fan then changes from a circular to rectangular cross section to mate with the fan output.

Inside the wheel housing, two ribbed, counter-rotating wheels connected to 10,000 RPM, 12 V motors rapidly accelerate the foam ball to 50 feet per second. Two ribbed wheels compress the ball from 23 mm to 14 mm to allow the wheels to grip tightly.

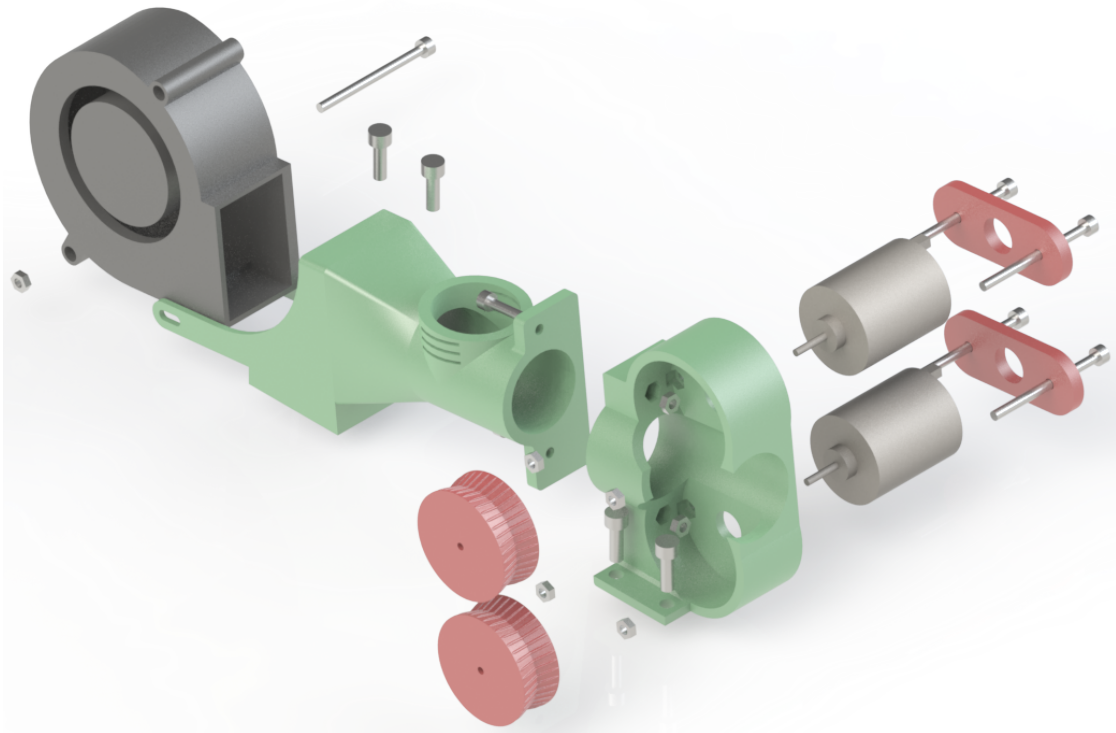


**Figure 2.5:** Shooting Mechanism – Exploded View

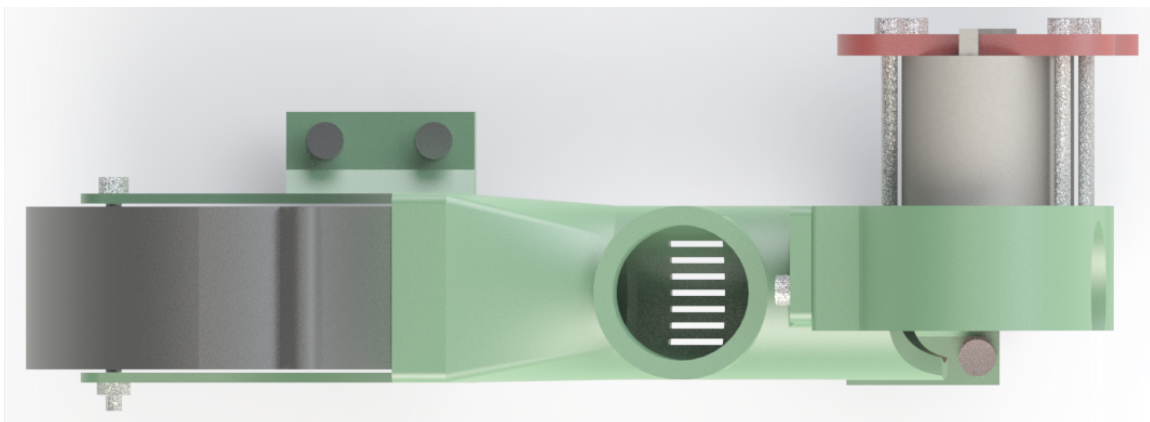


**Figure 2.6:** Shooting Mechanism – Top View

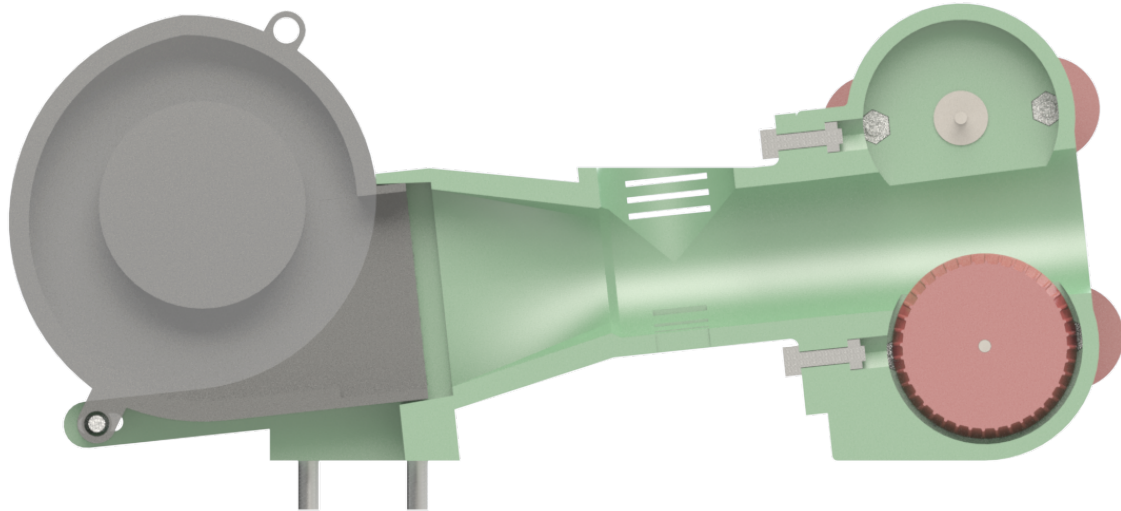


**Figure 2.7: Shooting Mechanism – Cross Section View**

An initial problem with the design was that the pressure created by the blower fan was so high that it prevented the ball from falling down the top chute. To alleviate the pressure while the ball is falling through the chute, vents were strategically placed to reduce the barrel pressure by allowing air to escape from more paths and causing turbulence. As the ball falls down into the barrel, it begins to cover and block the vents, increasing the pressure to allow the fan to push it out.

#### **2.4 Ball Hopper**

#### **2.5 Control Unit**

Chapter 3  
ELECTRICAL DESIGN

Chapter 4  
FIRMWARE DESIGN

## Chapter 5

### SOFTWARE

#### 5.1 Definitions and Assumptions

The robot is designed to only travel within a rectangular closed area of eight feet in the  $x$  direction and five feet in the  $y$  direction. The coordinate system is chosen as Cartesian with the origin placed at the bottom-left corner of the field. The position of the robot is always in the  $xy$ -plane since it cannot move vertically ( $z = 0$ ). Therefore,  $x$  refers to the robot position along the  $x$ -axis and ranges from 0 to 8 feet, and  $y$  refers to position along the  $y$ -axis and ranges from 0 to 5 feet. Additionally, the robot can only rotate around the  $z$ -axis so  $\theta$  refers to the angle of the robot in the  $xy$ -plane. Maintaining standard Cartesian coordinates,  $\theta = 0^\circ$  is along the positive  $x$  direction while  $\theta = 90^\circ$  is along the positive  $y$  direction.

#### 5.2 Kalman Filters

The system relies on several different sensors to determine where it is within the environment, a problem commonly referred to as robot localization. The *Kalman Filter* (KF), an optimal state estimator, performs noise filtering and sensor fusion, the process of combining measurements from multiple sensors. The filter operates on the principles of Bayesian inference and uses statistically noisy measurements over time and knowledge of the system to produce a more accurate estimate of an unknown variable than with measurement alone.

### 5.2.1 Algorithm

The Kalman Filter algorithm and equations are reproduced here from Roger Labbe's excellent interactive online book [3]. The algorithm consists of two stages (not including initialization): prediction and update. During the first stage, the filter uses the current state and a process model (typically a function of time) to estimate the state in the next time step along with its uncertainty. The second stage uses sensor measurements to update the estimation by taking a weighted average based on the ratio of uncertainty between the prediction and measurement.

#### Initialization

Before the first run of the filter, initialize the estimated state ( $\mathbf{x}$ , also called the posterior) and estimated state covariance matrix ( $\mathbf{P}$ ).

#### Predict

During the predict phase, the process model is used to predict the future state (known as the prior) ( $\bar{\mathbf{x}}$ ) after one time step by summing the posterior ( $\mathbf{x}$ ) multiplied by the *state transition function* ( $\mathbf{F}$ ) with the control input model ( $\mathbf{B}$ ) multiplied by the control input ( $\mathbf{u}$ ). The covariance of prior ( $\bar{\mathbf{P}}$ ) is larger than the posterior covariance ( $\mathbf{P}$ ) due to uncertainty in the process model ( $\mathbf{Q}$ ).

$$\bar{\mathbf{x}} = \mathbf{F}\mathbf{x} + \mathbf{B}\mathbf{u}$$

$$\bar{\mathbf{P}} = \mathbf{F}\mathbf{P}\mathbf{F}^T + \mathbf{Q}$$

## Update

Make measurements ( $\mathbf{z}$ , measurement mean) and determine their accuracy ( $\mathbf{R}$ , measurement noise covariance). Calculate the residual (or difference) ( $\mathbf{y}$ ) between the measurement and the product of the measurement function ( $\mathbf{H}$ ) and the prior from the previous phase.  $\mathbf{H}$  converts the prior from the state space to the measurement space. Calculate the weighting factor ( $\mathbf{K}$ , Kalman gain), valued between 0 and 1, based on the whether the measurement or prior is more accurate. Set the new posterior,  $\mathbf{x}$ , to an average of the measurement and prior, weighted by  $\mathbf{K}$ . Finally, update the posterior's covariance,  $\mathbf{P}$ , based on the measurement certainty. The algorithm then loops back to the predict phase using the newly-calculated posterior.

$$\mathbf{y} = \mathbf{z} - \mathbf{H}\bar{\mathbf{x}}$$

$$\mathbf{K} = \bar{\mathbf{P}}\mathbf{H}^T(\mathbf{H}\bar{\mathbf{P}}\mathbf{H}^T + \mathbf{R})^{-1}$$

$$\mathbf{x} = \bar{\mathbf{x}} + \mathbf{K}\mathbf{y}$$

$$\mathbf{P} = (\mathbf{I} - \mathbf{K}\mathbf{H})\bar{\mathbf{P}}$$

### 5.2.2 Design

The desired state variable  $\mathbf{x}$  is chosen as the linear position, velocity, and acceleration in the x and y directions as well as the angular position, velocity, and acceleration about the z-axis:

$$\mathbf{x} = [x \ y \ \theta]^T$$

$$\dot{\mathbf{x}} = [\dot{x} \ \dot{y} \ \dot{\theta}]^T$$

$$\ddot{\mathbf{x}} = [\ddot{x} \ \ddot{y} \ \ddot{\theta}]^T$$

The process model for position and velocity:

$$\begin{cases} \bar{x} = x + \dot{x}\Delta t + 0.5\ddot{x}(\Delta t)^2 \\ \dot{\bar{x}} = \dot{x} + \ddot{x}\Delta t \\ \ddot{\bar{x}} = \ddot{x} \end{cases}$$

Which can be written in the form:

$$\begin{bmatrix} \bar{x} \\ \dot{\bar{x}} \\ \ddot{\bar{x}} \end{bmatrix} = \begin{bmatrix} 1 & \Delta t & 0.5(\Delta t)^2 \\ 0 & 1 & \Delta t \\ 0 & 0 & 1 \end{bmatrix} \begin{bmatrix} x \\ \dot{x} \\ \ddot{x} \end{bmatrix}$$

$$\bar{\mathbf{x}} = \mathbf{F}\mathbf{x}$$

The measurement vector is chosen as:

$$\mathbf{z} = \begin{bmatrix} z_x & z_{\dot{x}} & z_y & z_{\ddot{x}} & z_{\theta} & z_{\dot{\theta}} \end{bmatrix}^T$$

The measurement noise matrix is shown below. The off-diagonals are 0 because the noise between sensors is assumed to be uncorrelated.

$$\mathbf{R} = \begin{bmatrix} \sigma_x^2 & 0 & 0 & 0 & 0 & 0 \\ 0 & \sigma_{\dot{x}}^2 & 0 & 0 & 0 & 0 \\ 0 & 0 & \sigma_y^2 & 0 & 0 & 0 \\ 0 & 0 & 0 & \sigma_{\ddot{x}}^2 & 0 & 0 \\ 0 & 0 & 0 & 0 & \sigma_{\theta}^2 & 0 \\ 0 & 0 & 0 & 0 & 0 & \sigma_{\dot{\theta}}^2 \end{bmatrix}$$

# Chapter 6

## NEURAL NETWORK DESIGN

## Chapter 7

### CONCLUSION

## BIBLIOGRAPHY

- [1] Cal Poly. Roborodentia - Cal Poly, San Luis Obispo. <http://www.myurl.com>, 2018. [Online; accessed May 11, 2018].
- [2] J. Doe. *The Book without Title*. Dummy Publisher, 2100.
- [3] R. R. Labbe. Kalman and Bayesian Filters in Python, Sep 2017.
- [4] R. Negenborn. *Robot Localization and Kalman Filters*. PhD thesis, Sep 2003.
- [5] D. H. Nguyen and B. Widrow. Neural Networks for Self-Learning Control Systems. *IEEE Control Systems Magazine*, Apr 1990.